ELSEVIER

Contents lists available at ScienceDirect

Science of the Total Environment

journal homepage: www.elsevier.com/locate/scitotenv





Novel staining—microscopy workflow visualizes microfibers in soil—plant systems: Implications for sustainable agriculture and food safety

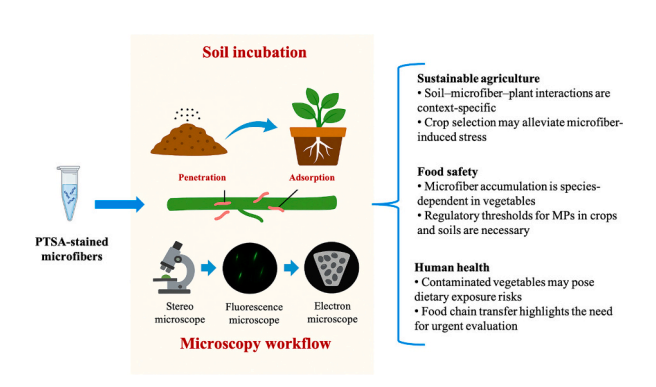
Zhangling Chen ^{a,b,*}, Laura J. Carter ^b, Steven A. Banwart ^a, Suruchi Roychoudhry ^c, Devlina Das Pramanik ^{d,e}, Paul Kay ^b

- ^a School of Earth and Environment, University of Leeds, Leeds, LS2 9JT, United Kingdom
- b School of Geography, University of Leeds, Leeds, LS2 9JT, United Kingdom
- ^c School of Biology, University of Leeds, Leeds, LS2 9JT, United Kingdom
- ^d School of Food Science and Nutrition, University of Leeds, Leeds, LS2 9JT, United Kingdom
- ^e Amity Institute of Biotechnology, Amity University Noida, Uttar Pradesh, 201313, India

HIGHLIGHTS

- PTSA staining enables clear visualization of MFs in complex soil-plant matrices.
- Species-specific MF adsorption was observed.
- MFs penetrate lettuce roots through crack-entry and apoplastic transport pathways.
- Root traits and antioxidant defenses regulate MF accumulation in edible plants.
- Crop selection may help mitigate risks in MF-contaminated agroecosystems.

G R A P H I C A L A B S T R A C T



ARTICLE INFO

Keywords:
Microfibers
Pollutant adsorption
Plant uptake
Fluorescence labeling
Microscopy
Agricultural sustainability
Food safety

ABSTRACT

Microfibers (MFs), primarily originating from sewage sludge and laundry effluents, are the most prevalent form of microplastics (MPs) in agricultural soils. While their ecological effects have been explored, the visualization, crop-level accumulation, and potential transport mechanisms of MFs within soil–plant systems remain poorly understood. This study combines 1,3,6,8-pyrene tetrasulfonic acid (PTSA) fluorescent staining with a sequential multimodal microscopy workflow to effectively track the distribution, adsorption, accumulation, and uptake of MFs under realistic soil cultivation conditions. Three edible vegetables—lettuce, Chinese cabbage, and cherry radish—were used to evaluate species-specific response patterns. The results revealed clear differences in MF interactions across species: lettuce exhibited strong MF adsorption on root surfaces and subsequent penetration via crack-entry and apoplastic pathways without entering cells. In contrast, Chinese cabbage and cherry radish showed limited MF adsorption and no uptake. These patterns were associated with root permeability and antioxidative capacities, indicating that plant functional traits play a critical role in determining the transport capacity of MPs. Beyond introducing a novel method for MF visualization in complex terrestrial matrices, this study provides new insights into the risks posed by MFs to soil-plant systems. The findings also highlight

^{*} Corresponding author at: School of Geography, University of Leeds, Leeds, LS2 9JT, United Kingdom. *E-mail address:* chenzhangling1101@gmail.com (Z. Chen).

Terminology used in this study for clarity:

- Distribution: dispersion of MFs within the soil or plant matrix.
- Adsorption / Adherence: attachment of MFs to the external surfaces of plant roots.
- **Penetration** / **Accumulation**: entry of MFs into root tissues, localizing in intercellular spaces without crossing cell membranes.
- **Uptake**: translocation of MFs across cell membranes into the symplast, potentially via endocytosis or plasmodesmata.

1. Introduction

Plastic production has increased exponentially since the mid-20th century, reaching 413.8 million metric tons globally in 2023 (Statista, 2025). However, inadequate disposal and low recycling rates have resulted in widespread plastic pollution, making it one of the most pressing environmental challenges worldwide (Zhang et al., 2022). Over time, larger plastic debris fragments into microplastics (MPs), defined as particles smaller than 5 mm (Thompson et al., 2004). While the occurrence, transport, and impacts of MPs in aquatic systems have been extensively studied, their behavior in terrestrial environments, particularly agricultural soils, remains relatively underexplored (Cheng et al., 2023). Agricultural lands, which cover nearly 38 % of the Earth's surface, are increasingly recognized as major reservoirs and potential sources of MPs (Yang et al., 2024). MPs can enter farmlands through multiple pathways, including plastic mulch degradation, sewage sludge application, wastewater irrigation, atmospheric deposition, littering, landfill leakage, and street runoff (Sahai et al., 2025; Brahney et al., 2020). Edible crops, which grow in direct contact with soil and water, are vulnerable to MP contamination. Previous studies have documented MP uptake in a range of species, including wheat, cucumber, oilseed rape, and Pak choi (Li et al., 2020; Li et al., 2021; Rong et al., 2024; Liu et al., 2025). Once incorporated into plant tissues, MPs can be transferred through the food chain, raising concerns for food safety and human health (Hou et al., 2025).

MPs can interact with plant roots through adsorption driven by electrostatic forces, hydrophobic interactions, or physical entanglement with root hairs (Xia et al., 2020). Once attached, smaller MPs (normally submicron and nano-scale) can penetrate root tissues via crack-entry sites, apoplastic transport, or symplastic pathways such as endocytosis and plasmodesmata-mediated movement (Li et al., 2020; Rong et al., 2024). Larger MPs (normally milli and micron-scale) typically remain adhered to the root surface, where they may hinder water and nutrient uptake (Chen et al., 2025a). However, much of the current evidence comes from hydroponic experiments, which tend to exhibit faster particle mobility and transpiration rates compared with soil-based systems (Khalid et al., 2020). Furthermore, many studies employ high exposure concentrations and use polystyrene microspheres (PS-MPs) with commercial fluorescent labels. While such approaches are useful for mechanistic and toxicological studies, they do not comprehensively reflect MP behavior in complex soil matrices, where diverse particle morphologies are present.

Among these morphologies, microfibers (MFs), which primarily originate from textile laundering and the application of compost or sludge, account for approximately 92 % of plastic particles in agricultural soils (Naderi Beni et al., 2023). Despite this prevalence, MF-plant interactions remain largely unstudied. Most current research on MP uptake by plants has focused on nanoscale PS-MPs, even though many MPs in farmland fall within the millimeter-to-micron size range (Yoon et al., 2024). Moreover, plant species and their root system architecture are likely to influence MP adsorption and transport. For example,

monocotyledonous plants (e.g., wheat and barley) and dicotyledonous plants (e.g., lettuce and carrot) have been shown to respond differently to MP exposure (Zantis et al., 2023). Some crops develop shallow fibrous root systems with abundant root hairs, others form deeper taproots with fewer lateral branches, and root-storage crops produce enlarged taproots specialized for nutrient accumulation. Such structural differences may lead to species-specific MP interactions (Chen et al., 2025b). Including multiple crop species is therefore essential for understanding interspecific variation in MP behavior and for improving the ecological relevance of risk assessments in agriculture.

To address these gaps, this study combined soil incubation experiments with advanced staining techniques and multimodal microscopy to track the fate of MFs in soil–plant systems. Lettuce (shallow root; leafy vegetable crop), Chinese cabbage (deep root; leafy vegetable crop), and cherry radish (root-storage; root vegetable crop) were selected as model crops to represent contrasting root architectures and edible tissues. We hypothesize that these structural differences may result in distinct patterns of MF adsorption, internal transport, and translocation efficiency. Using multiscale visualization, we aimed to characterize these patterns and provide new insights into MF dynamics, with broader implications for agricultural sustainability, food safety, and public health.

2. Materials and methods

2.1. Microfiber selection and processing

Polyester (PES) MFs were selected as the model MPs for this study. Fiber strands were procured from James Heal, United Kingdom. Initially, the MFs were manually cut with sharp scalpels and scissors to ensure their lengths were $<\!5\,\mathrm{mm}$. The fibers were then further processed using brushing and mechanical shredding techniques to generate micron-scale fibers. To eliminate potential microbial contaminants, the MFs were immersed in 10 % sodium hypochlorite (NaClO) for 5 min, thoroughly rinsed with deionized water to remove chemical residues, and dried on filter paper before use.

2.2. Microfiber staining and measurement

We selected 1,3,6,8-pyrene tetrasulfonate (PTSA) as the fluorescent dye because its hydrophilic anionic nature ensures stability and strong binding to polymeric surfaces without the need for organic solvents. Compared with commonly used dyes such as Nile red, PTSA offers lower background interference, making it advantageous for use in complex environmental samples (Pramanik et al., 2024). The attachment of PTSA to MFs occurs mainly through electrostatic interactions and hydrogen bonding between its sulfonate groups and polar functional groups on fiber surfaces. This binding is stable across a pH range of 4.1–9.1 and temperatures from 20 to 60 °C. Acute toxicity tests using *Artemia salina* have shown no significant adverse effects of PTSA, either alone or when bound to MFs (Pramanik et al., 2024). Collectively, these properties make PTSA suitable for tracking MFs in soil–plant systems, where high moisture content and complex matrix components often hinder conventional staining methods.

A concentrated PTSA solution was prepared by dissolving 5 mg PTSA in 80 mL deionized water. For staining, 250 μL of this stock solution was mixed with 50 mL deionized water and 8.88 g artificial seawater salts in amber Duran bottles. MFs were fully submerged in the mixture and stirred intermittently at 110 rpm for 24 h to ensure uniform staining. After staining, MFs were rinsed three times with deionized water to remove unbound dye and then dried on filter paper to minimize potential PTSA interference in subsequent soil–plant experiments. The

binding efficiency of PTSA to MFs was evaluated using an EVOS FL Auto 2 microscope, which confirmed no significant dye leakage (Fig. S1A). The size of MFs was determined from EVOS micrographs using ImageJ software, with an average length of 7.22 \pm 0.91 μm and an average diameter of 15.95 \pm 3.11 μm (Figs. S1B & S1C).

2.3. Soil preparation

Kettering loam soil was selected as the growth substrate due to its consistent texture, high nutrient retention capacity, and relevance in agricultural research (Botyanszká et al., 2022). The soil, sourced in 25 kg bags from Pitchcare, United Kingdom, was characterized by a pH of 6.8, an organic carbon content of 2.5 %, and a cation exchange capacity (CEC) of 18 cmol/kg. Before use, the soil was sieved through a 2 mm mesh, air-dried, and homogenized. MFs were incorporated into the soil by manual mixing in a tray to achieve uniform distribution.

2.4. Experimental setup

Lettuce (*Lactuca sativa*), Chinese cabbage (*Brassica rapa*), and cherry radish (*Raphanus sativus*) were selected as representative crops owing to their global agricultural relevance and suitability for standardized greenhouse cultivation. Lettuce was additionally included as a reference species, given its extensive use in contaminant uptake studies, which provides a robust baseline for comparison (Xu et al., 2023; Wang et al., 2021). By incorporating MFs into this study, we aimed to evaluate whether uptake pathways previously reported for PS-MPs also apply to MFs, and whether these trends are consistent across different crop species.

Seeds were obtained from Mr. Fothergill's (United Kingdom), surface-sterilized with 10 % NaClO for 5 min, and rinsed three times with deionized water to remove residual chemicals. After drying on filter paper, seeds were sown in glass jars (diameter: 8.5 cm; height: 9.4 cm) containing soil mixed with MFs at a concentration of 100 mg/kg. This concentration was chosen for two main reasons. First, it aligns with levels employed in previous hydroponic studies, where PS-MP uptake by plants was successfully observed (Zhou et al., 2021). Extending this dosage to soil-based experiments enables an assessment of whether similar uptake patterns occur in a more realistic agricultural medium. Second, Poisson regression modeling projects that MP concentrations in fertilized soils may rise to 168.9 mg/kg within the next 50 years (Meizoso-Regueira et al., 2024). Thus, 100 mg/kg represents both an experimentally validated and environmentally plausible exposure level, simulating potential near-future conditions and their long-term implications for soil-plant systems. Control groups consisted of jars without MFs (0 mg/kg), serving as a baseline for comparison with the treatment condition. Each group contained five biological replicates.

The experiment lasted 50 days under controlled greenhouse conditions, with a 12:12 h light–dark cycle and a constant temperature of 19 $^{\circ}$ C. Soil moisture was maintained through daily watering to prevent desiccation. At the end of the incubation period, all plants were harvested simultaneously (Fig. S2).

2.5. Application of multimodal microscopy

(1) Stereo microscopy

MFs in soil samples and on plant root surfaces were first screened using a Leica S6E stereomicroscope equipped with an external camera. Although the resolution of this system is relatively low, it provided a rapid preliminary assessment of MF presence and overall distribution.

(2) Fluorescence microscopy

For broader fluorescence-based screening, an EVOS FL Auto 2 microscope was applied. This wide-field system utilized a 4',6-diamidino-2-

phenylindole (DAPI) fluorescence filter cube (excitation ~357 nm, emission ~447 nm) to visualize PTSA-stained MFs, and a transmitted (Trans) light cube for non-fluorescent reference imaging of the same samples. Rhizosphere soil samples were collected with sterilized spatulas, stored in Petri dishes at 4 °C, and analyzed directly. Plant roots were excised with sterile scalpels, gently rinsed with deionized water, and hydrated prior to imaging. Samples that met predefined screening criteria were subsequently examined using a Zeiss LSM800 + Airyscan confocal laser scanning microscope (CLSM) for high-resolution and three-dimensional (3D) imaging. Roots were mounted in the Lab-Tek® Chambered #1.0 Borosilicate Coverglass System to ensure optimal positioning. Z-stack functionality was used to acquire serial optical sections along the Z-axis, which were computationally reconstructed into 3D models. This approach enabled virtual rotation and multi-angle visualization, revealing internal structures and MF spatial distribution. Fluorescence detection was performed in DAPI mode (excitation ~365 nm, emission ~445 nm) to visualize PTSA-stained MFs, while the transparent (ESID) mode provided non-fluorescent reference images of the same samples. Sample preparation followed the procedures described above.

(3) Electron microscopy

A FEI T12 transmission electron microscope equipped with a Lab6 filament and Gatan UltraScan 4000 CCD camera (TEM) was used for ultrastructural analysis. This technique was critical for confirming MF localization inside cellular compartments and for characterizing MF-tissue interactions at the subcellular level. Plant roots were cross-sectioned, fixed in glutaraldehyde and osmium tetroxide, dehydrated through a graded ethanol series, and embedded in epoxy resin. Ultrathin sections were then cut with a microtome and mounted on copper grids for imaging.

(4) Sequential imaging strategy and quality control

This stepwise workflow was designed to minimize unnecessary crosssection preparation, which is highly labor-intensive and resourcedemanding. The Leica S6E stereomicroscope and EVOS FL Auto 2 wide-field fluorescence microscope were therefore used only for preliminary screening, while CLSM and TEM were applied selectively to samples showing potential MF signals. This ensured that high-resolution imaging was conducted efficiently and only when justified. To reduce the risk of false-positive results, control soil and plant samples were examined under identical conditions. In some cases, DAPI-channel images appeared black because the samples either originated from control groups or from plant species that did not absorb MFs, and thus no fluorescence signal was activated under the DAPI filter. Images obtained in the Trans and ESID channels were also inherently non-fluorescent; MFs were often difficult to distinguish under these conditions, so these channels were used only as reference. This emphasized the necessity of PTSA staining to reliably differentiate MFs from soil-plant matrices. Fluorescence intensity in EVOS FL Auto 2 and CLSM images was assessed semi-quantitatively using a 0-3 scoring scale, where 0 = no visible fluorescence, 1 = weak, 2 = moderate, and 3 = strong. Scoring was performed independently by two blinded observers. For each treatment, five images were analyzed, and the mean \pm standard deviation (SD) was calculated. The scoring criteria and representative images for each fluorescence level are provided in the supplementary material (Text S1).

2.6. Auxiliary indicator test and statistical analysis

To complement the microscopic observations, several categories of auxiliary indicators were measured. First, soil bulk density and plant performance metrics (germination rate and total chlorophyll content) were assessed following the protocols described in our previous work (Chen et al., 2024). Second, oxidative stress biomarkers were evaluated

by measuring malondialdehyde (MDA) content, superoxide dismutase (SOD) activity, and the 2,2-diphenyl-1-picrylhydrazyl (DPPH) free radical scavenging rate. MDA content was used as an indicator of lipid peroxidation, SOD activity reflected the efficiency of the enzymatic antioxidant defense system, and the DPPH scavenging rate represented the capacity of the non-enzymatic antioxidant system. All biochemical assays were conducted using commercial kits obtained from Nanjing Jiancheng Bioengineering Institute, following the manufacturer's protocols (Texts S2-S4).

For statistical analysis, independent-samples t-tests were performed to compare differences between treatment groups using SPSS software. Prior to t-tests, normality was assessed using the Shapiro-Wilk test to ensure data conformed to a normal distribution. A threshold of p < 0.05 was considered statistically significant.

3. Results and discussion

3.1. Distribution of microfibers in rhizosphere soils

Microscopic analysis revealed that MFs adhered to soil particles and formed entanglements around them (Fig. 1). The distinctive characteristics of MFs, including high surface area, elongated shape, and flexibility, facilitate the formation of network-like structures within the soil matrix. These networks may promote the development of soil aggregates, as suggested by Xu et al. (2020), potentially enhancing structural stability and resistance to erosion by water and wind. Macroaggregates, according to previous studies, can harbor more diverse and active microbial communities, which may contribute to enhanced nutrient cycling and organic carbon stabilization (Chen et al., 2024). Such stabilization may in turn slow the decomposition of soil organic matter and potentially contribute to climate change mitigation (Han et al., 2024).

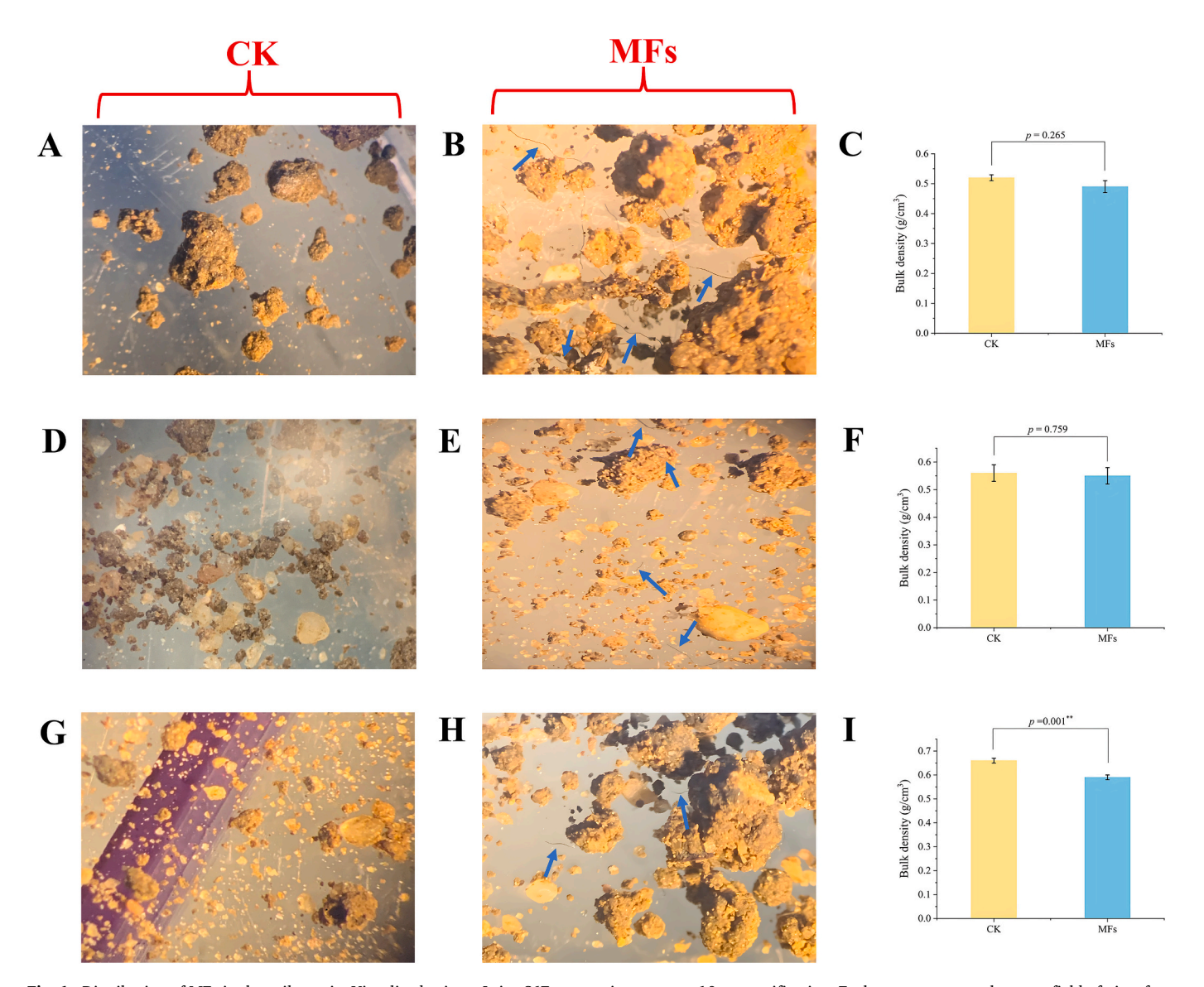


Fig. 1. Distribution of MFs in the soil matrix. Visualized using a Leica S6E stereomicroscope at $10 \times$ magnification. Each row represents the same field of view for a given treatment. (A,B) Lettuce-growing soil; (D,E) Chinese cabbage-growing soil; (G,H) Cherry radish-growing soil. Bulk density values for the corresponding soils are shown in (C,F,I).

- [1] Representative images are selected from five analyzed samples per treatment.
- [2] CK: Control treatment without MFs; MFs: Treatment with 100 mg/kg PTSA-stained MFs.
- [3] Blue arrows indicate the presence of MFs. The Leica S6E is a stereomicroscope, and MFs observed with this technique do not show fluorescence signals.
- [4] For t-test results, data are presented as mean \pm standard error (SE), N=5.
- [5] Statistical significance is indicated as follows: p < 0.01 (**).

However, MFs can also cause undesirable changes in soil physical properties. In our study, MFs significantly reduced soil bulk density, particularly in cherry radish-growing soils (p < 0.05; Fig. 1I), corroborating previous findings that MF contamination leads to a looser soil structure (de Souza Machado et al., 2018). While reduced bulk density may enhance soil aeration, it often impairs water retention capacity and overall soil productivity (Yu et al., 2023). Additionally, increased porosity may create textural discontinuities that hinder root penetration and disrupt root-soil interactions (Correa et al., 2019). These structural alterations can influence water dynamics and nutrient availability, both of which are important for soil health and crop performance (de Souza Machado et al., 2019). In drought-prone regions, such changes may be particularly concerning, since reduced water-holding capacity (WHC) could require more frequent irrigation, posing potential challenges to water resource management and agricultural sustainability, as suggested by Lozano and Rillig (2020).

The dual nature of MF-soil interactions, involving potential aggregation enhancement but also the compromise of certain physical properties, highlights the complexity of their effects on soil quality. Balancing these opposing impacts should be a priority for future research, especially given the anticipated rise in agro-MP pollution in the coming decades.

3.2. Fluorescent visualization of microfibers in the soil matrix

Fluorescence tracking is widely used for detecting MPs in soil–plant systems, but its accuracy is often hampered by background fluorescence from natural organic matter in soil and plant tissues, particularly when fluorescent PS-MPs are used (Hua et al., 2023). This background noise can create uncertainty in identifying MPs within complex matrices. To address this challenge, we applied PTSA dye staining for the first time in a soil–plant context, and MFs were clearly distinguishable from the background, helping to mitigate interference from natural fluorescence (Fig. 2).

MFs are an important source of MP contamination in agroecosystems, with emissions estimated at 124–308 mg per kg of clothing washed (De Falco et al., 2019). Biosolid amendments further contribute to MF accumulation, with fibers constituting up to 97 % of all plastic particles in agricultural soils (Corradini et al., 2019). Despite their prevalence, detecting MFs remains challenging due to their flexible morphology and the heterogeneity of environmental matrices (Ingraffia et al., 2022). In our study, images from the Trans non-fluorescent channel served as references, where MFs could not be readily distinguished from surrounding soil particles (Fig. 2B, E, and H). By contrast, PTSA staining enabled reliable visualization of MFs within the soil matrix under DAPI fluorescent channel (Fig. 2C, F, and I), highlighting

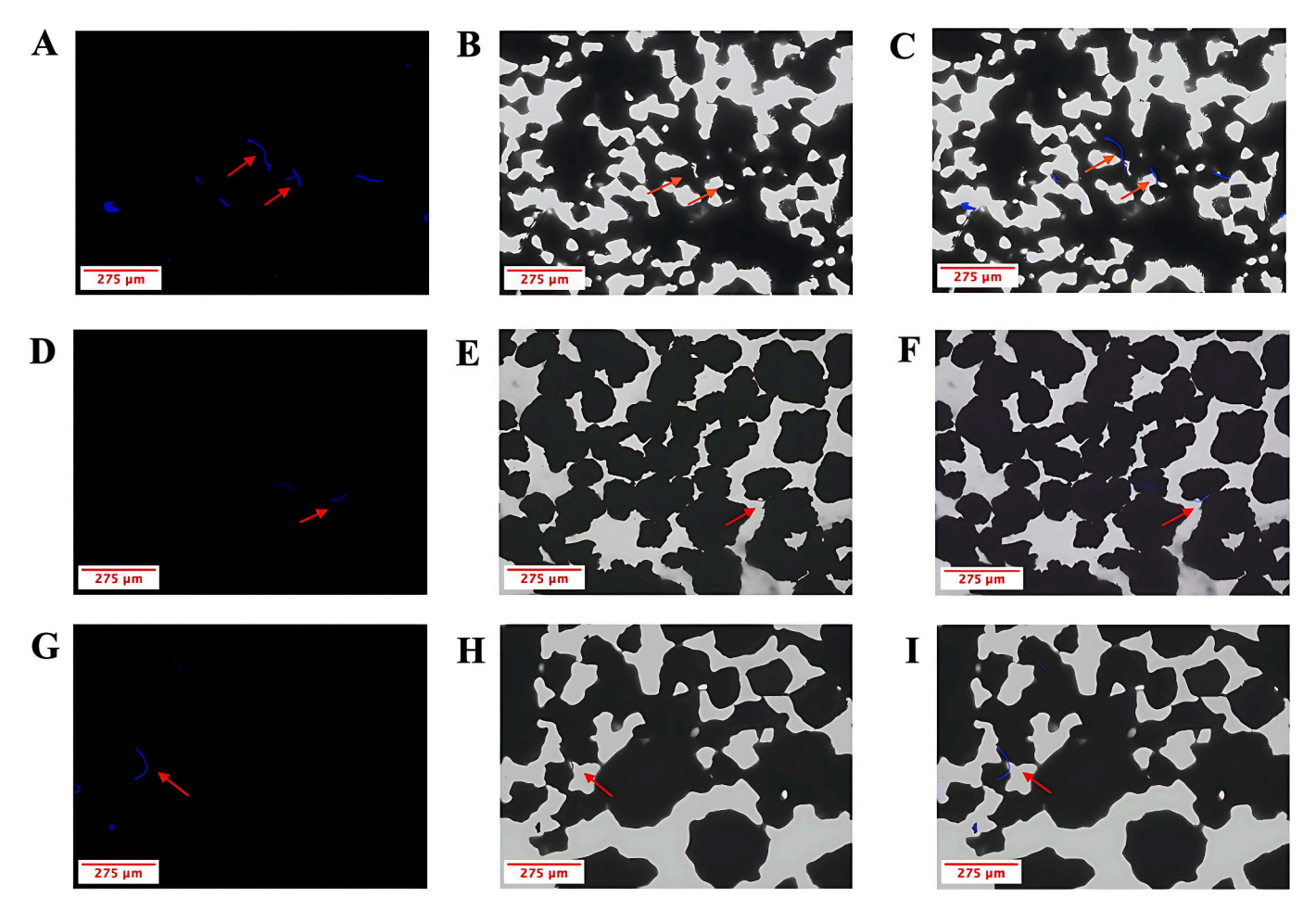


Fig. 2. Distribution of MFs in the soil matrix. Visualized using the EVOS FL Auto 2 microscope: scale bar $= 275 \,\mu m$. Each row represents the same field of view for a given treatment. (A-C) Lettuce-growing soil; (D—F) Chinese cabbage-growing soil; (G–I) Cherry radish-growing soil. Images in (A, D, G) were captured using the DAPI (fluorescent) light cube; (B, E, H) were captured using the Trans (non-fluorescent) light cube; and (C, F, I) show merged images from the DAPI and Trans light cubes.

- [1] Representative images are selected from five analyzed samples per treatment.
- [2] Red arrows indicate the presence of PTSA-stained MFs.
- [3] Control soil samples (0 mg/kg) for each vegetable type are shown in Fig. S3 for comparison and to avoid false-positive results.
- [4] The Trans channel does not generate fluorescence signals; therefore, MFs in images B, E, and H appear black (MF's original color).

its potential as a tool for future studies on MF interactions with soil biota, nutrient cycling, and crop systems. This approach may also contribute to agricultural safety evaluations and environmental risk assessments.

Nevertheless, several limitations should be acknowledged. The shredding process generated MFs with heterogeneous lengths and diameters, and some fragments were so short that they appeared only as small fluorescent spots in microscope images. Although such particles could be localized with the EVOS FL Auto 2 microscope, their dimensions could not be accurately quantified using ImageJ. Because particle size is known to strongly influence MP migration and interactions, future studies should adopt advanced imaging approaches combined with specialized analysis software, such as FiberApp, to enable precise characterization of smaller MFs (Chen et al., 2025a). Another limitation concerns the co-occurrence of MPs with other soil contaminants, which may cause additional signal interference and is

likely to remain a persistent technical challenge (Wang et al., 2023). Furthermore, the potential leaching of PTSA during long-term experiments, and its subsequent effects on soil and plant health, should also be considered. Direct measurement of PTSA in soil leachates, for instance, would provide more definitive evidence of its stability.

3.3. Species-specific patterns of microfiber adsorption on plant root surfaces

Leica S6E stereomicroscope observations showed that MFs adhered to and wrapped around the root surfaces of lettuce and Chinese cabbage. Adsorption was more pronounced in lettuce (Fig. 3B), whereas Chinese cabbage exhibited lower adsorption (Fig. 3E). These results are consistent with earlier reports of 2 μ m PS-MPs adhering to lettuce roots (Li et al., 2020). Fluorescence imaging with the EVOS FL Auto 2 further confirmed species-specific adsorption patterns. In lettuce, MFs were

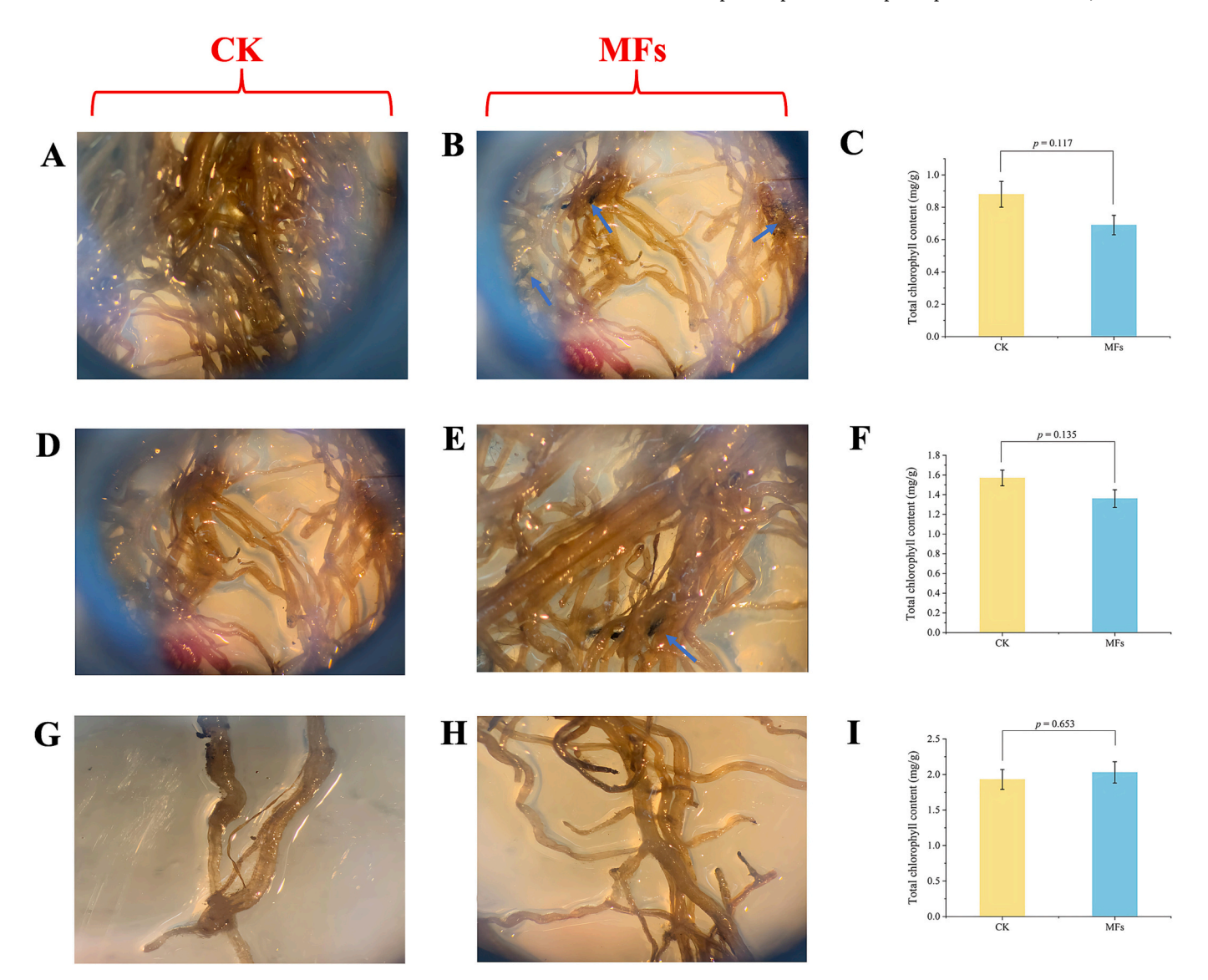


Fig. 3. Adsorption of MFs on plant root surfaces. Visualized using a Leica S6E stereomicroscope at $10 \times$ magnification. Each row represents the same field of view for a given treatment. (A, B) Lettuce root; (D, E) Chinese cabbage root; (G, H) Cherry radish root. Total chlorophyll content values for the corresponding plants are shown in (C, F, I).

- [1] Representative images are selected from five analyzed samples per treatment.
- [2] CK: Control treatment without MFs; MFs: Treatment with 100 mg/kg PTSA-stained MFs.
- [3] Blue arrows indicate the presence of MFs, no MFs were detected on cherry radish root surfaces. The Leica S6E is a stereomicroscope, and MFs observed with this technique do not show fluorescence signals.
- [4] For t-test results, data are presented as mean \pm standard error (SE), N=5.

primarily localized on the main root, with only sparse presence on lateral roots (Figs. 4A-4F). In contrast, Chinese cabbage retained only small amounts of MFs, exclusively on the main root (Figs. 4G-4I). No detectable MFs were observed on cherry radish roots using either microscopy technique (Fig. 3H and Fig. S4). The distinct adsorption patterns may be attributable to differences in root structural traits and antioxidant responses. In lettuce, larger intercellular spaces and more permeable epidermal layers may facilitate MF entanglement (Yu et al., 2024). In addition, a relatively high cellulose content on its root surface may promote hydrophilic interactions with MFs (Wang et al., 2022a). In contrast, the lower MF adhesion in Chinese cabbage may be explained by less favorable root surface properties or by more active antioxidant defenses, as suggested by its higher enzyme activity detected in this study (p < 0.05; Fig. 6F). For cherry radish, the absence of detectable MF adsorption is likely related to its root morphology; as the taproot enlarges into a storage organ, lateral roots become sparse, thereby reducing the total root surface area available for MF contact (Chen et al., 2025b).

MF adsorption on root surfaces has been linked to a cascade of physiological and biochemical stress responses. Jia et al. (2023) reported that MPs can disrupt the root epidermis, triggering defense pathways and stimulating the production of reactive oxygen species (ROS). Elevated ROS levels compromise cellular integrity, disturb ionic

balance, and increase membrane permeability (Chen et al., 2025b). Such root-level disturbances can propagate systemically and lead to measurable changes in aboveground tissues. In our study, significant alterations in antioxidant enzyme activity were observed in the leaves of lettuce and Chinese cabbage exposed to MFs (p < 0.05; Figs. 5J and 6F). These findings are consistent with Sun et al. (2024), who showed that plants typically respond to oxidative stress by enhancing antioxidant defenses. Similar responses have also been reported under other abiotic stressors, such as pH fluctuations, temperature shifts, and heavy metal exposure, all of which elevate MDA levels and reduce chlorophyll content (Wang et al., 2022b; Akpinar and Cansev, 2024). In line with these findings, we observed a significant increase in MDA levels (p < 0.05; Fig. 5I) and a decreasing trend in total chlorophyll content (p > 0.05; Fig. 3C) in lettuce following MF exposure. Ceccanti et al. (2024) further suggested that MPs on root surfaces may hinder water and nutrient transport between roots and the rhizosphere, including uptake of magnesium and iron, which are essential cofactors for chlorophyll biosynthesis. This mechanism may partly explain the chlorophyll decline observed here.

In addition to these physiological and biochemical responses, macroscale growth indicators offered further insights into MF-plant interactions. Early-stage germination data showed that MF exposure promoted seed germination in lettuce and Chinese cabbage compared with the control (Fig. S5). This effect may be linked to MF-induced

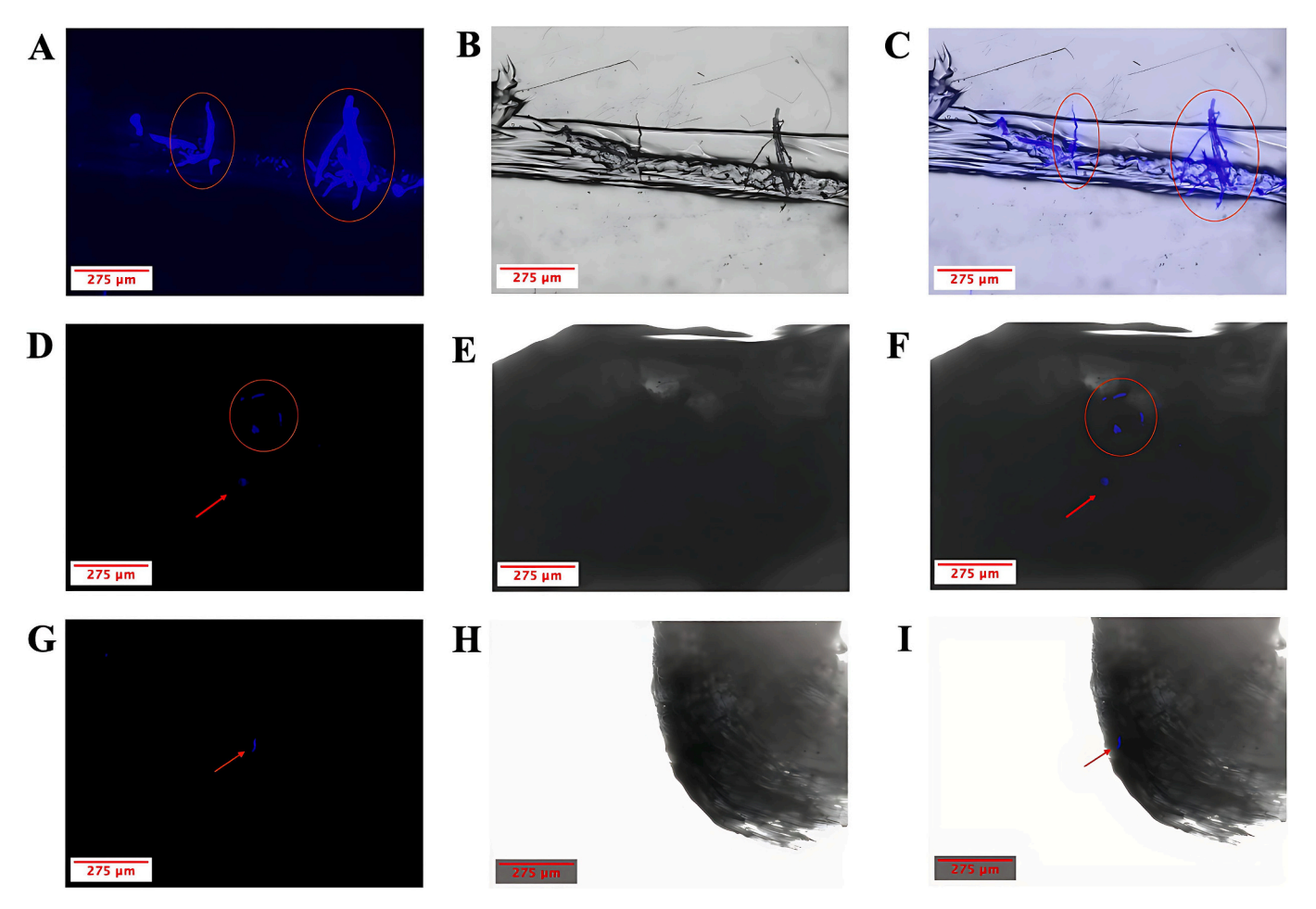


Fig. 4. Adsorption of MFs in lettuce and Chinese cabbage root surfaces. Visualized using the EVOS FL Auto 2 microscope: scale bar $= 275 \mu m$. Each row represents the same field of view for a given treatment. (A–C) Lettuce main root; (D—F) Lettuce lateral root; (G–I) Chinese cabbage main root. Images in (A, D, G) were captured using the DAPI (fluorescent) light cube; (B, E, H) were captured using the Trans (non-fluorescent) light cube; and (C, F, I) show merged images from the DAPI and Trans light cubes.

- [1] Representative images are selected from five analyzed samples per treatment.
- [2] Red circles and arrows indicate the presence of PTSA-stained MFs.
- [3] Control plant samples (0 mg/kg) for each vegetable type are shown in Fig. S4 for comparison and to avoid false-positive results.
- [4] The Trans channel does not generate fluorescence signals; therefore, MFs in images B, E, and H appear black (MF's original color).

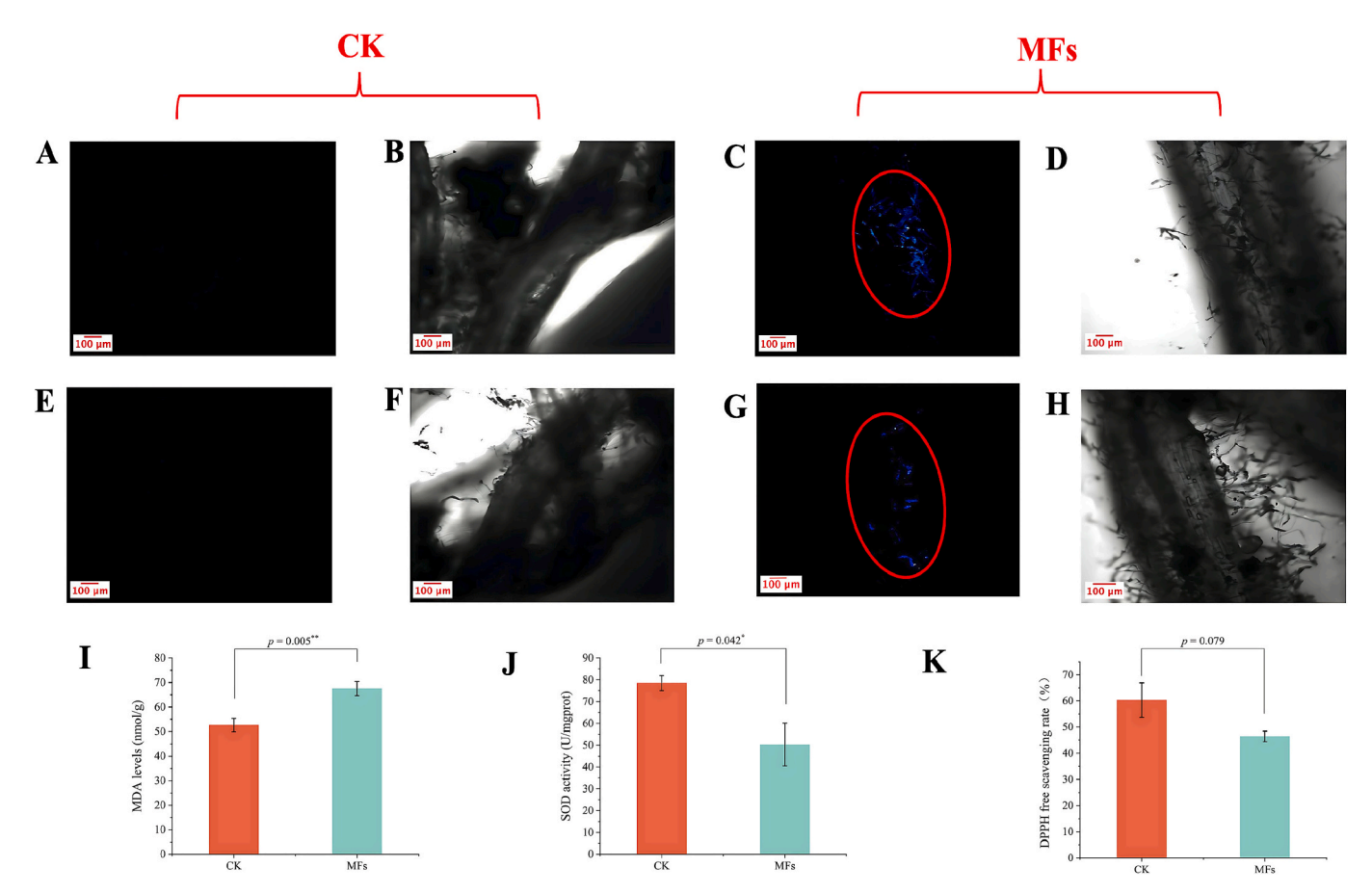


Fig. 5. Penetration of MFs in lettuce roots. Visualized using the Zeiss LSM 800 Upright Confocal Microscope with Z stack functionality: scale bar = 100 μm. (A–B) Lettuce main root-Control treatment; (C–D) Lettuce main root-Microfiber treatment; (E-F) Lettuce lateral root-Control treatment. (G-H) Lettuce lateral root-Microfiber treatment. Images in (A, C, E, G) were captured using the DAPI (fluorescent) light cube; (B, D, F, H) were captured using the ESID (non-fluorescent) light cube. MDA levels, SOD activity, and DPPH free scavenging rates values for the lettuce samples are shown in (I, J, K).

- [1] Representative images are selected from five analyzed samples per treatment.
- [2] CK: Control treatment without MFs; MFs: Treatment with 100 mg/kg PTSA-stained MFs.
- [3] Red circles indicate the presence of PTSA-stained MFs.
- [4] In control samples, images acquired with the DAPI channel appear black because no MFs were added and thus no fluorescence signal was activated. Images A and E are provided for comparison and to avoid false-positive interpretation.
- [5] The ESID channel does not produce fluorescence signals; therefore, MFs in images B, D, F, and H appear black, reflecting their original black color.
- [6] For t-test results, data are presented as mean \pm standard error (SE), with N = 5.
- [7] Statistical significance is indicated as follows: p < 0.05 (*), p < 0.01 (**).

changes in soil physical properties, such as reduced bulk density and increased porosity, which can enhance water infiltration and aeration around seeds (Chen et al., 2024). However, these initial benefits did not translate into long-term advantages; prolonged MF exposure was associated with declines in chlorophyll content and shifts in oxidative stress markers. Collectively, these results indicate that while MFs may confer short-term stimulation under certain conditions, their long-term presence poses risks to crop health and productivity. Moreover, the magnitude of these effects varied among crop species, underscoring the need for future studies that integrate root anatomical traits and surface properties to elucidate species-specific response mechanisms. Such knowledge is critical for predicting crop tolerance and vulnerability under MF contamination. From an applied perspective, varieties with inherently lower MF adsorption may be more suitable for cultivation in contaminated soils. Incorporating these traits into breeding and selection programs could therefore contribute to broader strategies aimed at reducing contamination risks and promoting sustainable agricultural production.

3.4. Penetration and localization of microfibers within plant roots

Z-stack optical sectioning and 3D reconstruction using CLSM revealed the spatial distribution of MFs within root tissues. Fluorescence signals were detected in both the main and lateral roots of lettuce, with the latter showing weaker signals than the former (Fig. 5C and G). No signals were observed in the control group under DAPI light tube (Fig. 5A and E), confirming that the fluorescence originated from PTSAstained MFs and indicating the penetration of MFs into lettuce roots. In contrast, no fluorescence was detected in Chinese cabbage under the same conditions (Figs. 6A-6D), suggesting that MFs did not enter its root tissues. As cherry radish roots showed no surface-level MF adsorption, CLSM imaging was not conducted for this species. TEM images provided further evidence of MF localization. No MFs were detected inside lettuce root cells (Fig. 7); instead, they were confined to the apoplastic space, suggesting that penetration occurred through crack-entry and apoplastic transport rather than symplastic uptake. Taken together, these results provide the first direct evidence of MF penetration into the roots of edible crops, extending previous studies that primarily examined the internalization of spherical PS-MPs.

Several structural factors may explain the penetration observed in

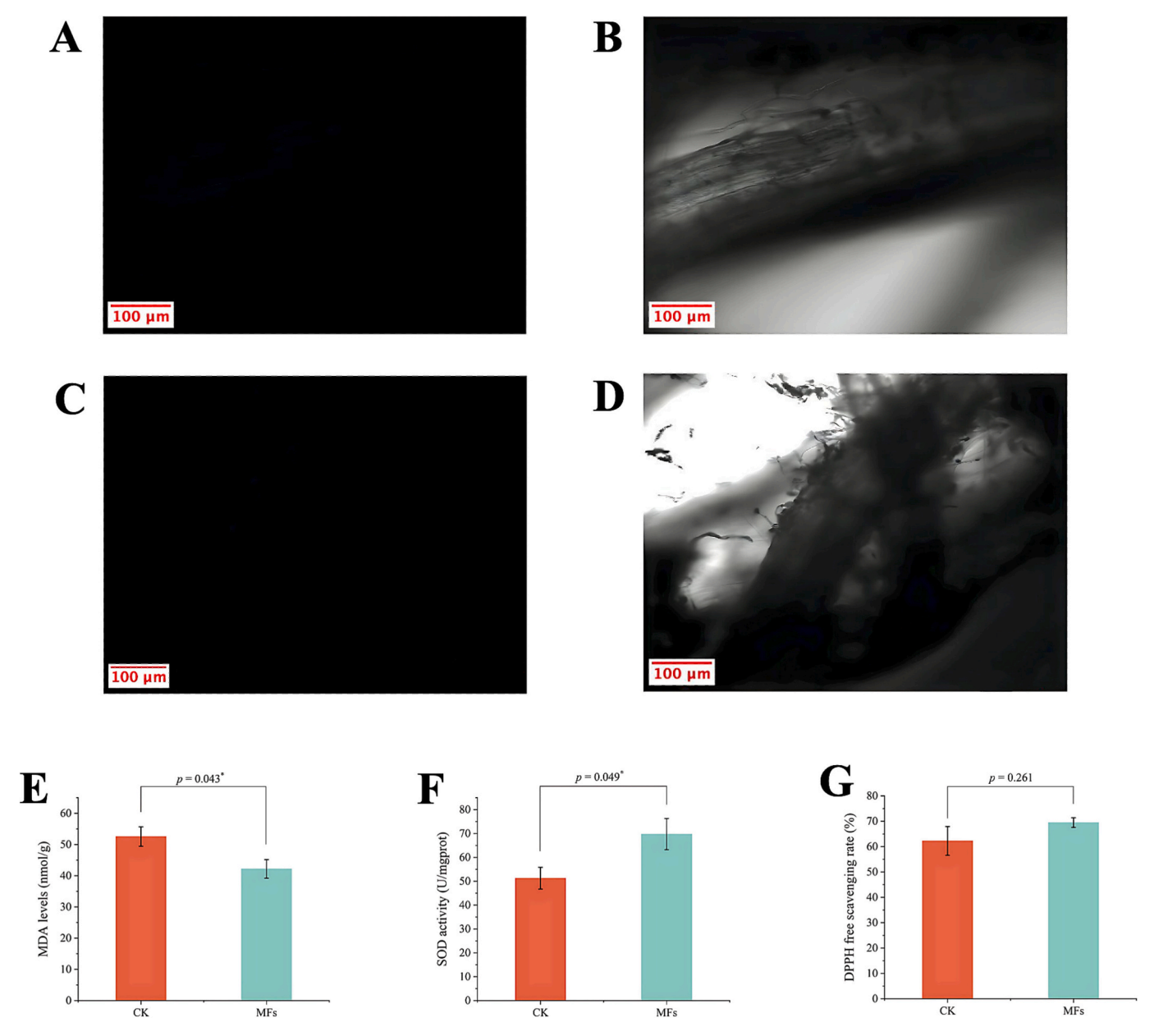


Fig. 6. Penetration of MFs in Chinese cabbage roots. Visualized using the Zeiss LSM 800 Upright Confocal Microscope with Z stack functionality: scale bar = 100 μm. (A–B) Chinese cabbage main root-Control treatment; (C—D) Chinese cabbage main root-Microfiber treatments. Images in (A, C) were captured using the DAPI (fluorescent) light cube; (B, D) were captured using the ESID (non-fluorescent) light cube. MDA levels, SOD activity, and DPPH free scavenging rates values for the Chinese cabbage samples are shown in (E, F, G).

- [1] Representative images are selected from five analyzed samples per treatment.
- [2] CK: Control treatment without MFs; MFs: Treatment with 100 mg/kg PTSA-stained MFs.
- [3] In control samples, Image A acquired with the DAPI channel appear black because no MFs were added and thus no fluorescence signal was activated. It is provided for comparison and to avoid false-positive interpretation.
- [4] In positive samples, Image C acquired with the DAPI channel appear black because no MFs were detected and thus no fluorescence signal was activated.
- [5] The ESID channel does not produce fluorescence signals; therefore, MFs in images B and D appear black, reflecting their original black color.
- [6] For t-test results, data are presented as mean \pm standard error (SE), with N = 5.
- [7] Statistical significance is indicated as follows: p < 0.05 (*).

lettuce. Microfissures naturally formed during root elongation can serve as entry points, while the high aspect ratio and flexibility of MFs may allow them to align with and traverse these fissures (Li et al., 2020). In addition, the hydrophilic surface chemistry of MPs has been suggested to enhance adhesion to root surfaces and mobility in the rhizosphere (Xu et al., 2024). Greater root permeability in lettuce has also been reported to facilitate apoplastic entry, and rhizospheric fluid dynamics together with mechanical forces generated during root growth could further promote MF transport into tissues (Wang et al., 2022b). Physiological

measurements can also help explain the differences in penetration between lettuce and Chinese cabbage. In lettuce, MF exposure was associated with a significant increase in MDA content (p < 0.01), a significant decrease in SOD activity (p < 0.05), and a decreasing trend in DPPH radical scavenging capacity (p > 0.05) (Figs. 5I–5K), indicating reduced antioxidative capacity. By contrast, Chinese cabbage showed a significant decrease in MDA content (p < 0.05), a significant increase in SOD activity (p < 0.05), and an increasing trend in DPPH radical scavenging capacity (p > 0.05) (Figs. 6E–6G), suggesting an enhanced

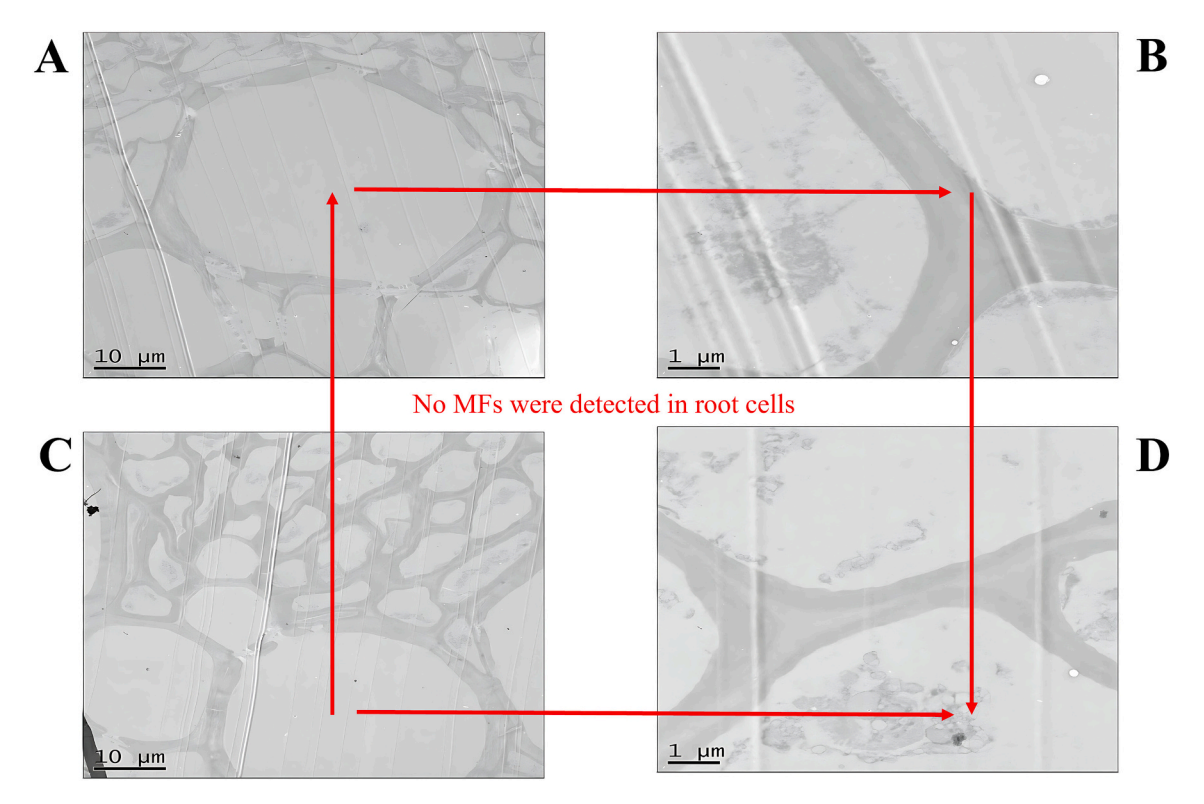


Fig. 7. Localization of MFs in lettuce root cells. Visualized using the TEM, scale bar $= 10 \mu m$, $1 \mu m$. Each row represents the same field of view for a given treatment. (A–B) Lettuce main root-Control treatment; (C–D) Lettuce main root-Microfiber treatment.

- [1] Representative images are selected from five analyzed samples per treatment.
- [2] TEM does not produce fluorescence signals.
- [3] No MFs were observed with this technique.

antioxidative response. Previous studies have reported that ROS-induced lipid peroxidation can impair root membrane integrity and increase intercellular permeability, thereby facilitating particle entry (Chang et al., 2024). In lettuce, reduced SOD activity may have weakened ROS scavenging, compromising root barrier function. Moreover, oxidative stress has been suggested to alter root exudation, enhancing secretion of organic acids and phenolic compounds that modify MP surface charge and retention at the root interface (Teterovska et al., 2023). Stress-induced changes in root hair density and morphology may further increase attachment sites and promote penetration (Zhang et al., 2023). Although membrane lipid peroxidation was assessed through MDA content in this study, future work incorporating electrolyte leakage assays could provide more direct evidence of membrane integrity and help clarify the physiological mechanisms underlying MF penetration or uptake.

Although MFs were not detected in aboveground tissues such as lettuce leaves, Chinese cabbage leaves, or cherry radish taproots, their persistence in root systems raises potential food safety concerns. Under prolonged exposure or under different environmental conditions, translocation to edible organs may still occur, particularly when roots or contaminated soil are inadvertently ingested. Future studies should therefore investigate (1) whether extended exposure or more severe contamination facilitates MF movement from roots to edible tissues, (2) whether crops with different edible parts (roots vs. leaves) differ in exposure risk, and (3) the potential health implications of dietary MP intake. Despite these uncertainties, our study highlights the need for precautionary strategies, including the establishment of regulatory thresholds for MP contamination in agricultural soils and food products, as well as guidelines for crop selection in contaminated farmland.

Field investigations further demonstrate that MP contamination in agricultural soils is already widespread, particularly in sludge-amended fields. Reported concentrations range from 545.9 and 87.6 particles/kg

following annual sludge applications of 30 t/ha and 15 t/ha, respectively, to 3500 particles/kg in soils with cumulative sludge inputs of 200 t/ha (Zhang et al., 2020; Corradini et al., 2019). These values are generally lower than the 100 mg/kg applied in this study; however, localized hotspots or long-term intensive sludge application may lead to substantially higher accumulation. The concentration chosen here was primarily intended to validate the microscopy workflow and simulate scenarios of prolonged, severe contamination. Nonetheless, reliance on a single high concentration does not reflect typical background levels or permit the evaluation of dose–response relationships. Future studies should therefore incorporate contamination gradients to better capture plant adsorption and uptake under realistic field conditions, thereby supporting more comprehensive agricultural risk assessments.

3.5. A sequential microscopy workflow to visualize microfibers in soil-plant systems

To systematically track the fate of MFs in soil–plant systems, we developed a sequential microscopy workflow that integrates multiple imaging modalities in a stepwise, decision-based manner (Fig. 8). This approach ensures that high-resolution, resource-intensive techniques are applied only when necessary, thereby improving efficiency and minimizing unnecessary workload. Importantly, the workflow provides a scalable strategy that can be adapted by researchers with different levels of resources to maximize visualization of MPs in complex matrices.

The workflow proceeds through four sequential stages. First, the Leica S6E stereomicroscope provides a macroscopic survey of MF distribution at the soil–root interface, capturing large-scale interactions between soil particles, roots, and MFs, though its relatively low resolution limits detection of finer fibers. Next, the EVOS FL Auto 2 fluorescence microscope serves as a rapid screening tool, enabling high-

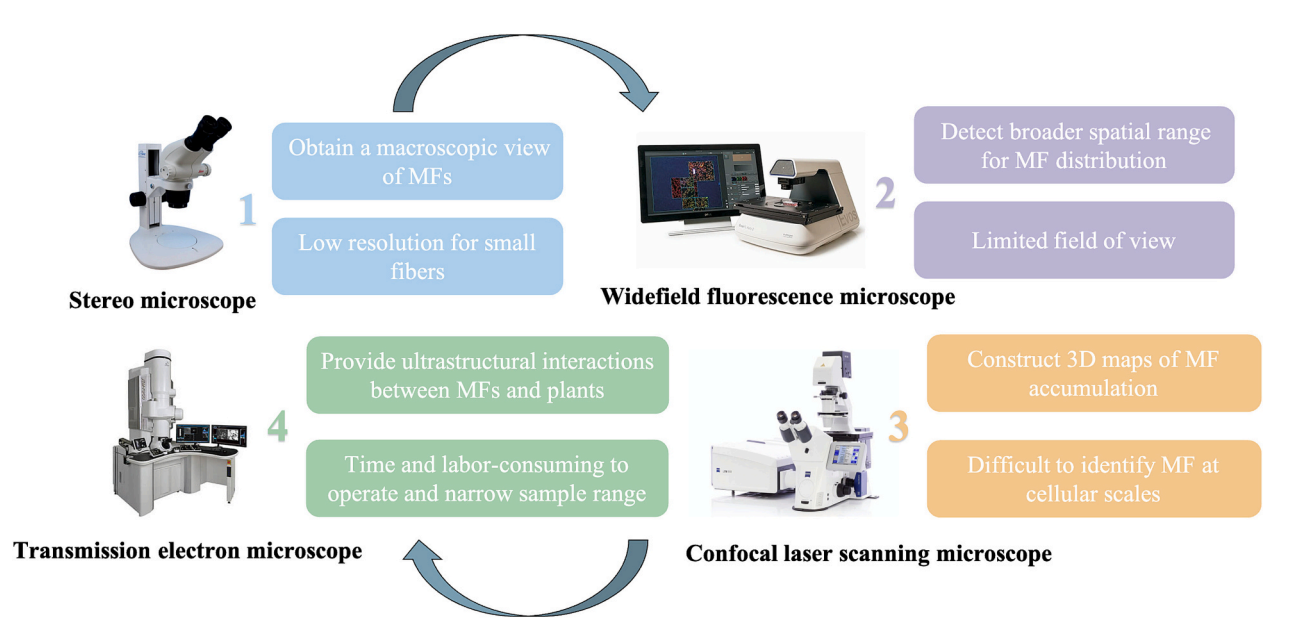


Fig. 8. Sequential microscopy workflow for tracking MF fate in soil-plant systems.

contrast detection of PTSA-stained MFs across wide fields of view; however, its limited depth view makes it unsuitable for internal localization. Samples with potential MF presence are then examined using CLSM, where Z-stack optical sectioning generates 3D reconstructions of penetration pathways and accumulation sites, balancing resolution, throughput, and tissue preservation. Finally, TEM provides ultrastructural confirmation of MF localization at cellular and subcellular scales. Although TEM offers the highest spatial resolution, it requires destructive ultrathin sectioning and was therefore reserved for cases where earlier steps indicated likely MF presence. The application of this workflow across the three plant species is summarized in Table 1.

Several methodological refinements supported the workflow, including the use of organic fluorophores, chambered coverglass systems, and automated Z-stack imaging, which together enhanced the precision of MF visualization in both soil and plant samples. Rather than replacing conventional methods, this tiered approach offers a robust and adaptable framework for studying MP dynamics in agroecosystems. Future research should strengthen cross-validation protocols between stages and integrate imaging with biochemical and molecular analyses to better elucidate the mechanisms of MP adsorption, accumulation, and translocation in crops.

4. Conclusion

MFs are the dominant form of MPs in agricultural soils, yet their behavior in soil-plant systems remains insufficiently understood. In this study, we developed a sequential multimodal microscopy workflow combined with PTSA staining to enhance the detection and visualization of MFs in complex soil-plant matrices. This methodological advancement extends fluorescence-based techniques beyond the commonly studied spherical PS-MPs and enables more accurate assessment of MF distribution and accumulation in terrestrial ecosystems. Our results revealed clear species-specific differences in MF adsorption and accumulation. Lettuce roots showed strong surface fluorescence and evidence of internal penetration via crack-entry and apoplastic pathways, although no MFs were observed inside cells. Chinese cabbage exhibited weaker surface adsorption and no internal uptake, while cherry radish displayed neither surface nor internal accumulation. These variations may reflect differences in root structural traits and antioxidative capacity among species. From an environmental risk perspective, the adhesion of MFs to roots and their potential transfer to edible tissues

 $\begin{tabular}{ll} \textbf{Table 1}\\ \textbf{Summary of microscopy techniques applied to different plant species in this study.}\\ \end{tabular}$

Microscopy technique	Lettuce	Chinese cabbage	Cherry radish
Leica S6E stereromicroscope	√	√	√
EVOS FL Auto 2 flurescence microscope	√	√	√
Confocal laser scanning microscope	√	√	×
Transmission electron microscope	√	×	×

raise concerns for food safety and human exposure through the food chain. These findings underscore the need for regulatory frameworks to define acceptable MP levels in agricultural soils and food products. At the same time, the observed interspecies variation highlights crop selection as a possible mitigation strategy. Cultivating plant varieties with stronger physiological defenses may help reduce MP accumulation in food crops and contribute to more sustainable agroecosystems under growing plastic pollution pressures.

CRediT authorship contribution statement

Zhangling Chen: Writing – review & editing, Writing – original draft, Software, Methodology, Investigation, Formal analysis, Conceptualization. Laura J. Carter: Writing – review & editing, Supervision. Steven A. Banwart: Supervision, Funding acquisition. Suruchi Roychoudhry: Methodology, Formal analysis. Devlina Das Pramanik: Software, Methodology. Paul Kay: Writing – review & editing, Supervision, Funding acquisition.

Declaration of competing interest

The authors declare that they have no known competing financial interests or personal relationships that could have appeared to influence the work reported in this paper.

Acknowledgements

The authors express their sincere gratitude to the School of Earth and Environment and the School of Geography at the University of Leeds for their support in providing the experimental funding for this research. Special thanks are also extended to the staff at the School of Geography's

Laboratory (Rachel Gasior, David Ashley, Joshua Greenwood, and Holly Armitage), the School of Molecular and Cellular Biology (Martin Fuller), as well as the Bio-imaging and Flow Cytometry Facility (Ruth Hughes and Sally Boxall), at the University of Leeds for their invaluable technical assistance.

Appendix A. Supplementary data

Supplementary data to this article can be found online at https://doi. org/10.1016/j.scitotenv.2025.180671.

Data availability

Data will be made available on request.

References

- Akpinar, A., Cansev, A., 2024. Choline supplementation reduces cadmium uptake and alleviates cadmium toxicity in Solanum lycopersicum seedlings. BMC Plant Biol. 24 (1). https://doi.org/10.1186/s12870-024-05653-w, 977.
- Botyanszká, L., Šurda, P., Vitková, J., Lichner, L., Igaz, D., 2022. Effect of microplastics on silty loam soil properties and radish growth. Journal of Hydrology and Hydromechanics 70 (3), 321–329. https://doi.org/10.2478/johh-2022-0018.
- Brahney, J., Hallerud, M., Heim, E., Hahnenberger, M., Sukumaran, S., 2020. Plastic rain in protected areas of the United States. Science (American Association for the Advancement of Science) 368 (6496), 1257–1260. https://doi.org/10.1126/science. aaz5819.
- Ceccanti, C., Davini, A., Lo Piccolo, E., Lauria, G., Rossi, V., Ruffini Castiglione, M., Spanò, C., Bottega, S., Guidi, L., Landi, M., 2024. Polyethylene microplastics alter root functionality and affect strawberry plant physiology and fruit quality traits. J. Hazard. Mater. 470, 134164. https://doi.org/10.1016/j.jhazmat.2024.134164.
- Chang, N., Chen, L., Wang, N., Cui, Q., Qiu, T., Zhao, S., He, H., Zeng, Y., Dai, W., Duan, C., Fang, L., 2024. Unveiling the impacts of microplastic pollution on soil health: a comprehensive review. Sci. Total Environ. 951, 175643. https://doi.org/ 10.1016/j.scitotenv.2024.175643.
- Chen, Z., Carter, L.J., Banwart, S.A., Pramanik, D.D., Kay, P., 2024. Multifaceted effects of microplastics on soil-plant systems: exploring the role of particle type and plant species. Sci. Total Environ. 954, 176641. https://doi.org/10.1016/j. scitoteny. 2024.176641.
- Chen, Z., Carter, L.J., Banwart, S.A., Kay, P., 2025a. Microplastics in Soil–Plant Systems: Current Knowledge, Research Gaps, and Future Directions for Agricultural Sustainability. Agronomy (Basel) 15 (7), 1519. https://doi.org/10.3390/ agronomy15071519.
- Chen, Z., Carter, L.J., Banwart, S.A., Kay, P., 2025b. Environmental levels of microplastics disrupt growth and stress pathways in edible crops via species-specific mechanisms. Front. Plant Sci. 16, 1670247. https://doi.org/10.3389/ fpls.2025.1670247.
- Cheng, J., Meistertzheim, A.-L., Leistenschneider, D., Philip, L., Jacquin, J., Escande, M.-L., Barbe, V., ter Halle, A., Chapron, L., Lartaud, F., Bertrand, S., Escriva, H., Ghiglione, J.-F., 2023. Impacts of microplastics and the associated plastisphere on physiological, biochemical, genetic expression and gut microbiota of the filter-feeder amphioxus. Environ. Int. 172, 107750-. https://doi.org/10.1016/j.envint.2023.107750.
- Corradini, F., Meza, P., Eguiluz, R., Casado, F., Huerta-Lwanga, E., Geissen, V., 2019. Evidence of microplastic accumulation in agricultural soils from sewage sludge disposal. Sci. Total Environ. 671, 411–420. https://doi.org/10.1016/j. scitotenv.2019.03.368.
- Correa, J., Postma, J.A., Watt, M., Wojciechowski, T., Zhang, J., 2019. Soil compaction and the architectural plasticity of root systems. J. Exp. Bot. 70 (21), 6019–6034. https://doi.org/10.1093/jxb/erz383.
- De Falco, F., Di Pace, E., Cocca, M., Avella, M., 2019. The contribution of washing processes of synthetic clothes to microplastic pollution. Sci. Rep. 9 (1), 6633. https://doi.org/10.1038/s41598-019-43023-x.
- de Souza Machado, A.A., Lau, C.W., Till, J., Kloas, W., Lehmann, A., Becker, R., Rillig, M. C., 2018. Impacts of microplastics on the soil biophysical environment. Environ. Sci. Technol. 52 (17), 9656–9665. https://doi.org/10.1021/acs.est.8b02212.
- de Souza Machado, A.A., Lau, C.W., Kloas, W., Bergmann, J., Bachelier, J.B., Faltin, E., Becker, R., Görlich, A.S., Rillig, M.C., 2019. Microplastics can change soil properties and affect plant performance. Environ. Sci. Technol. 53 (10), 6044–6052. https://doi.org/10.1021/acs.est.9b01339.
- Han, L., Chen, L., Feng, Y., Kuzyakov, Y., Chen, Q., Zhang, S., Chao, L., Cai, Y., Ma, C., Sun, K., Rillig, M.C., 2024. Microplastics alter soil structure and microbial community composition. Environ. Int. 185, 108508. https://doi.org/10.1016/j.envint.2024.108508.
- Hou, L., Fu, Y., Zhao, C., Fan, L., Hu, H., Yin, S., 2025. Short-term exposure to ciprofloxacin and microplastic leads to intrahepatic cholestasis, while long-term exposure decreases energy metabolism and increases the risk of obesity. Environ. Int. 199, 109511-. https://doi.org/10.1016/j.envint.2025.109511.
 Hua, Z., Ma, S., Ouyang, Z., Liu, P., Qiang, H., Guo, X., 2023. The review of nanoplastics
- Hua, Z., Ma, S., Ouyang, Z., Liu, P., Qiang, H., Guo, X., 2023. The review of nanoplastics in plants: detection, analysis, uptake, migration and risk. TrAC, Trends in Analytical Chemistry (Regular Ed.) 158, 116889. https://doi.org/10.1016/j.trac.2022.116889.

- Ingraffia, R., Amato, G., Bagarello, V., Carollo, F.G., Giambalvo, D., Iovino, M., Lehmann, A., Rillig, M.C., Frenda, A.S., 2022. Polyester microplastic fibers affect soil physical properties and erosion as a function of soil type. Soil 8 (1), 421–435. https://doi.org/10.5194/soil-8-421-2022.
- Jia, L., Liu, L., Zhang, Y., Fu, W., Liu, X., Wang, Q., Tanveer, M., Huang, L., 2023. Microplastic stress in plants: effects on plant growth and their remediations. Front. Plant Sci. 14, 1226484. https://doi.org/10.3389/fpls.2023.1226484.
- Khalid, N., Aqeel, M., Noman, A., 2020. Microplastics could be a threat to plants in terrestrial systems directly or indirectly. Environmental Pollution 267 (1987). https://doi.org/10.1016/j.envpol.2020.115653, 115653-.
- Li, L., Luo, Y., Li, R., Zhou, Q., Peijnenburg, W.J.G.M., Yin, N., Yang, J., Tu, C., Zhang, Y., 2020. Effective uptake of submicrometre plastics by crop plants via a crack-entry mode. Nature Sustainability 3 (11), 929–937. https://doi.org/10.1038/s41893-020-0567.0
- Li, Z., Li, Q., Li, R., Zhou, J., Wang, G., 2021. The distribution and impact of polystyrene nanoplastics on cucumber plants. Environ. Sci. Pollut. Res. Int. 28 (13), 16042–16053. https://doi.org/10.1007/s11356-020-11702-2.
- Liu, Z., Qin, M., Li, R., Peijnenburg, W.J.G.M., Yang, L., Liu, P., Shi, Q., 2025. Transport dynamics and physiological responses of polystyrene Nanoplastics in Pakchoi: implications for food safety and environmental health. J. Agric. Food Chem. 73 (18), 10923–10933. https://doi.org/10.1021/acs.jafc.5c03590.
- Lozano, Y.M., Rillig, M.C., 2020. Effects of microplastic fibers and drought on plant communities. Environ. Sci. Technol. 54 (10), 6166–6173. https://doi.org/10.1021/ acs.est.0c01051.
- Meizoso-Regueira, T., Fuentes, J., Cusworth, S.J., Rillig, M.C., 2024. Prediction of future microplastic accumulation in agricultural soils. Environ. Pollut. 1987 (359), 124587. https://doi.org/10.1016/j.envpol.2024.124587.
- Naderi Beni, N., Karimifard, S., Gilley, J., Messer, T., Schmidt, A., Bartelt-Hunt, S., 2023. Higher concentrations of microplastics in runoff from biosolid-amended croplands than manure-amended croplands. Commun. Earth Environ. 4 (1), 42–49. https:// doi.org/10.1038/s43247-023-00691-y.
- Pramanik, D.D., Kay, P., Goycoolea, F.M., 2024. A rapid and portable fluorescence spectroscopy staining method for the detection of plastic microfibers in water. Sci. Total Environ. 908, 168144. https://doi.org/10.1016/j.scitotenv.2023.168144.
- Rong, S., Wang, S., Liu, H., Li, Y., Huang, J., Wang, W., Han, B., Su, S., Liu, W., 2024. Evidence for the transportation of aggregated microplastics in the symplast pathway of oilseed rape roots and their impact on plant growth. Sci. Total Environ. 912, 169419. https://doi.org/10.1016/j.scitotenv.2023.169419.
- Sahai, H., Aguilera del Real, A.M., Alcayde, A., Bueno, M.J.M., Wang, C., Hernando, M. D., Fernández- Alba, A.R., 2025. Key insights into microplastic pollution in agricultural soils: a comprehensive review of worldwide trends, sources, distribution, characteristics and analytical approaches. TrAC, Trends in Analytical Chemistry (Regular Ed.) 185, 118176. https://doi.org/10.1016/j.trac.2025.118176.
- Statista, 2025. Annual production of plastics worldwide from 1950 to 2023. https://www.statista.com/statistics/282732/global-production-of-plastics-since-1950/. Accessed 5 March 2025.
- Sun, X., Xiao, T., Qin, J., Song, Y., Lu, K., Ding, R., Shi, W., Bian, Q., 2024. Mechanism of circRNA_SMG6 mediating lung macrophage ECM degradation via miR-570-3p in microplastics-induced emphysema. Environ. Int. 187, 108701-. https://doi.org/ 10.1016/j.envirt.2024.108701
- Teterovska, R., Sile, I., Paulausks, A., Kovalcuka, L., Koka, R., Mauriņa, B., Bandere, D., 2023. The antioxidant activity of wild-growing plants containing phenolic compounds in Latvia. Plants (Basel) 12 (24), 4108. https://doi.org/10.3390/plants12244108.
- Thompson, R.C., Olsen, Y., Mitchell, R.P., Davis, A., Rowland, S.J., John, Anthony W.G., McGonigle, D., Russell, A.E., 2004. Lost at sea: where is all the plastic? Science (American Association for the Advancement of Science) 304 (5672), 838. https://doi.org/10.1126/science.1094559.
- Wang, F., Wang, X., Song, N., 2021. Polyethylene microplastics increase cadmium uptake in lettuce (Lactuca sativa L.) by altering the soil microenvironment. Sci. Total Environ. 784, 147133. https://doi.org/10.1016/j.scitotenv.2021.147133.
- Wang, F., Feng, X., Liu, Y., Adams, C.A., Sun, Y., Zhang, S., 2022a. Micro(nano)plastics and terrestrial plants: up-to-date knowledge on uptake, translocation, and phytotoxicity. Resour. Conserv. Recycl. 185, 106503. https://doi.org/10.1016/j. rescource 2022 106503
- Wang, J., Tao, J., Ji, J., Wu, M., Sun, Y., Li, J., Gan, J., 2023. Use of a dual-labeled bioaccumulation method to quantify microplastic vector effects for hydrophobic organic contaminants in soil. ACS Environmental Au 3 (4), 233–241. https://doi. org/10.1021/acsenvironau.3c00024.
- Wang, W., Yuan, S., Kwon, J.-H., 2022b. Insight into the uptake and translocation of perand polyfluoroalkyl substances in hydroponically grown lettuce. Environ. Sci. Pollut. Res. Int. 29 (56), 85454–85464. https://doi.org/10.1007/s11356-022-21886-4.
- Xia, Y., Zhou, J.-J., Gong, Y.-Y., Li, Z.-J., Zeng, E.Y., 2020. Strong influence of surfactants on virgin hydrophobic microplastics adsorbing ionic organic pollutants. Environmental Pollution 1987 (265). https://doi.org/10.1016/j. envpol.2020.115061 (Pt B), Article 115061.
- Xu, B., Liu, F., Cryder, Z., Huang, D., Lu, Z., He, Y., Wang, H., Lu, Z., Brookes, P.C., Tang, C., Gan, J., Xu, J., 2020. Microplastics in the soil environment: occurrence, risks, interactions and fate a review. Crit. Rev. Environ. Sci. Technol. 50 (21), 2175–2222. https://doi.org/10.1080/10643389.2019.1694822.
- Xu, G., Lin, X., Yu, Y., 2023. Different effects and mechanisms of polystyrene. micro- and nano-plastics on the uptake of heavy metals (cu, Zn, Pb and cd) by lettuce (Lactuca sativa L.). Environ. Pollut. 1987 (316). https://doi.org/10.1016/j.envpol.2022.120656 (Pt 2), 120656-.

- Xu, Y., Ou, Q., van der Hoek, J.P., Liu, G., Lompe, K.M., 2024. Photo-oxidation of Microand Nanoplastics: physical, chemical, and biological effects in environments. Environ. Sci. Technol. 58 (2), 991–1009. https://doi.org/10.1021/acs.est.3c07035.
- Yang, X., Wan, Z., Xiao, J., Li, F., Zhang, F., Zhang, Z., 2024. Evaluation of niche, diversity, and risks of microplastics in farmland soils of different rocky desertification areas. J. Hazard. Mater. 466, 133603. https://doi.org/10.1016/j. jhazmat.2024.133603.
- Yoon, J.-H., Kim, B.-H., Kim, K.-H., 2024. Distribution of microplastics in soil by. Types of land use in metropolitan area of Seoul. *Applied*. Biol. Chem. 67 (1). https://doi.org/10.1186/s13765-024-00869-8, 15-13.
- Yu, Y., Battu, A.K., Varga, T., Denny, A.C., Zahid, T.M., Chowdhury, I., Flury, M., 2023. Minimal impacts of microplastics on soil physical properties under environmentally relevant concentrations. Environ. Sci. Technol. 57 (13), 5296–5304. https://doi.org/ 10.1021/acs.est.2c09822.
- Yu, Z., Xu, X., Guo, L., Jin, R., Lu, Y., 2024. Uptake and transport of micro/nanoplastics in terrestrial plants: detection, mechanisms, and influencing factors. Sci. Total Environ. 907, 168155. https://doi.org/10.1016/j.scitotenv.2023.168155.

- Zantis, L.J., Rombach, A., Adamczyk, S., Velmala, S.M., Adamczyk, B., Vijver, M.G., Peijnenburg, W., Bosker, T., 2023. Species-dependent responses of crop plants to polystyrene microplastics. Environ. Pollut. 1987 (335). https://doi.org/10.1016/j. envpol.2023.122243 article 122243.
- Zhang, L., Xie, Y., Liu, J., Zhong, S., Qian, Y., Gao, P., 2020. An overlooked entry pathway of microplastics into agricultural soils from application of sludge-based fertilizers. Environ. Sci. Technol. 54 (7), 4248–4255. https://doi.org/10.1021/acs. est 9b07905
- Zhang, Y., Yang, Z., Zhang, Z., Li, Y., Guo, J., Liu, L., Wang, C., Fan, H., Wang, B., Han, G., 2023. Root hair development and adaptation to abiotic stress. J. Agric. Food Chem. 71 (25), 9573–9598. https://doi.org/10.1021/acs.jafc.2c07741.
- Zhang, Z., Cui, Q., Chen, L., Zhu, X., Zhao, S., Duan, C., Zhang, X., Song, D., Fang, L., 2022. A critical review of microplastics in the soil-plant system: distribution, uptake, phytotoxicity and prevention. J. Hazard. Mater. 424 (Pt D), 127750. https://doi.org/ 10.1016/j.jhazmat.2021.127750.
- Zhou, C.-Q., Lu, C.-H., Mai, L., Bao, L.-J., Liu, L.-Y., Zeng, E.Y., 2021. Response of rice (Oryza sativa L.) roots to nanoplastic treatment at seedling stage. J. Hazard. Mater. 401, 123412. https://doi.org/10.1016/j.jhazmat.2020.123412.